3D wave propagation simulations of the 2019 M7.1 Ridgecrest, CA, Earthquake

Te-Yang Yeh[1,2] and Kim Bak Olsen[1]

[1]Department of Geological Sciences, San Diego State University

[2]IGPP, Scripps Institution of Oceanography, University of California, San Diego

San Diego State University
Department of Geological Sciences
College of Sciences

Cecil H. and Ida M. Green Institute of Geophysics and Planetary Physics
IGPP

SCEC
AN NSF+USGS CENTER

This research was supported by the Southern California Earthquake Center (Contribution No.11626). SCEC is funded by NSF Cooperative Agreement EAR-1600087 and USGS Cooperative Agreement G17AC00047.

An award of computer time was provided by the INCITE program. This research used resources of the Oak Ridge Leadership Computing Facility, which is a DOE Office of Science User Facility supported under Contract DE-AC05-00OR22725.

Objectives

Analyze the contribution of scattering from topography and small-scale heterogeneities (SSHs) on the ground motions recorded from the 2019 M7.1 Ridgecrest earthquake at high frequencies (> 1 Hz).

Numerical modeling

- Simulations were carried out on OLCF Summit using the simulation code AWP-ODC-GPU-TOPO (O'Reilly et al., 2021)
- Grid spacing: 25m
- Domain size: 7992 x 5994 x 3200 grid points
- Minimum Vs: 500 m/s
- Maximum frequency: 3Hz
- Velocity model: SCEC UCVM CVM-S4.26.M01 (with built-in GTL)
- Anelastic attenuation model:

$$Qs = 0.1Vs \text{ for } f \leq 1Hz$$

$$Qs(f) = 0.1Vs(\frac{f}{f_0})^{0.6} \text{ for } f > 1Hz$$

$$Qp = 2Qs$$

- Topography model: USGS Southern California DEM 3-arc-second resolution

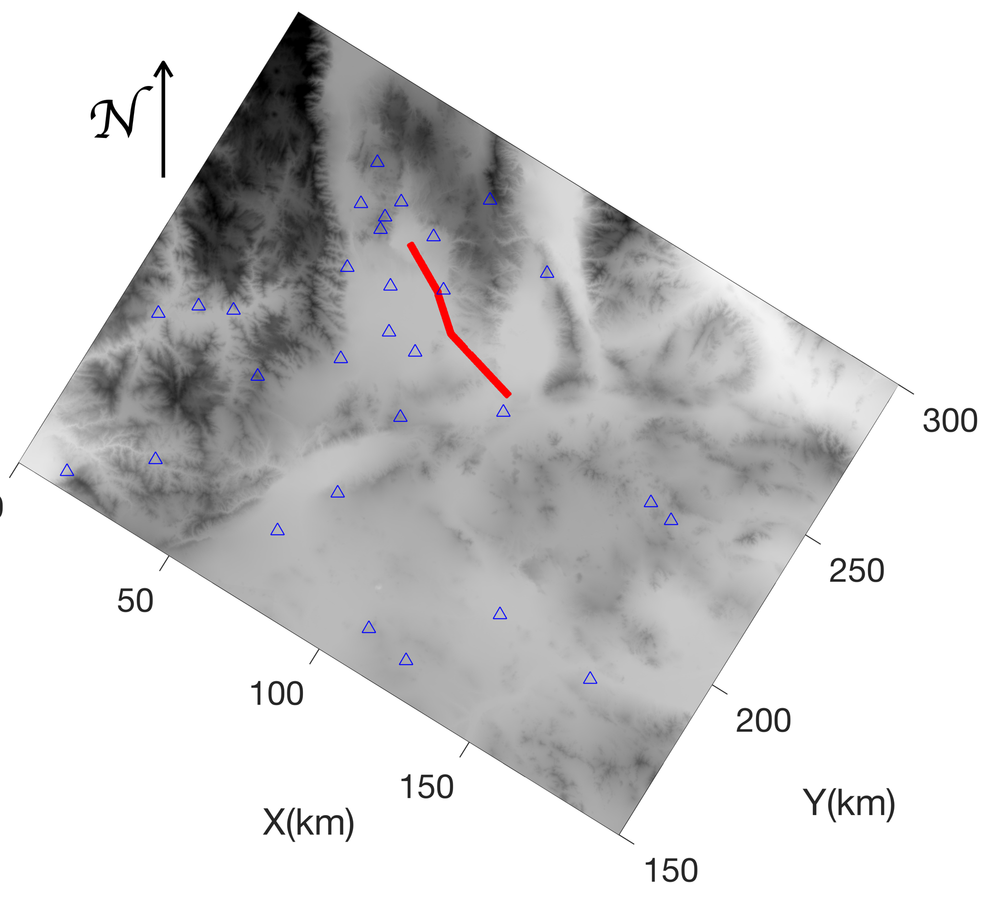

Map of the simulation domain. Gray shading depicts the topographic elevation. The red lines show the location of the 3-segment finite-fault model. Blue triangles are location of strong motion stations used to validate the synthetic ground motions.

Source model

We first acquired slip rate functions for the finite-fault rupture model by Liu et al., (2019) inverted from seismic and geodetic data. The inverted source rupture models mainly represent low frequency source response due to limited resolution of source imaging. Using the procedure demonstrated in Figure (a) below, we perturbed the moment rate function of each subfault by multiplying it with von Karman correlated noise to enhance the high-frequency energy, such that the total source spectrum matches a targeted source spectrum of the form:

$$M(f) = \frac{M_0}{1 + (f/fc)^n}$$

We grid search to estimate the optimal correlation time (Tc) and standard deviation (σ) of the von Karman noise until the total spectrum follows the targeted high-frequency decay (assuming n=2 in this case, as shown in Figure c). Meanwhile, the total moment rate function after the enhancement remains close to the unperturbed one (Figure b).

(a)

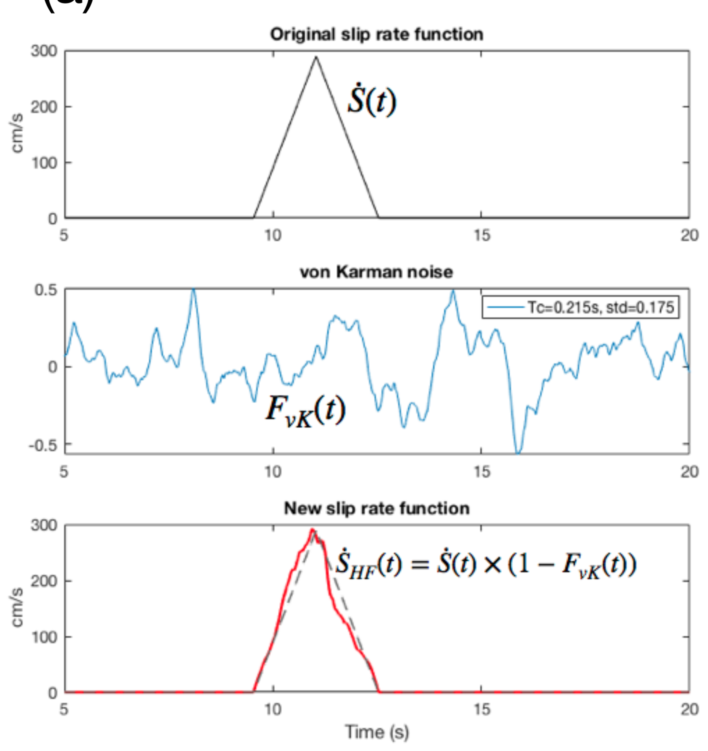

(b)

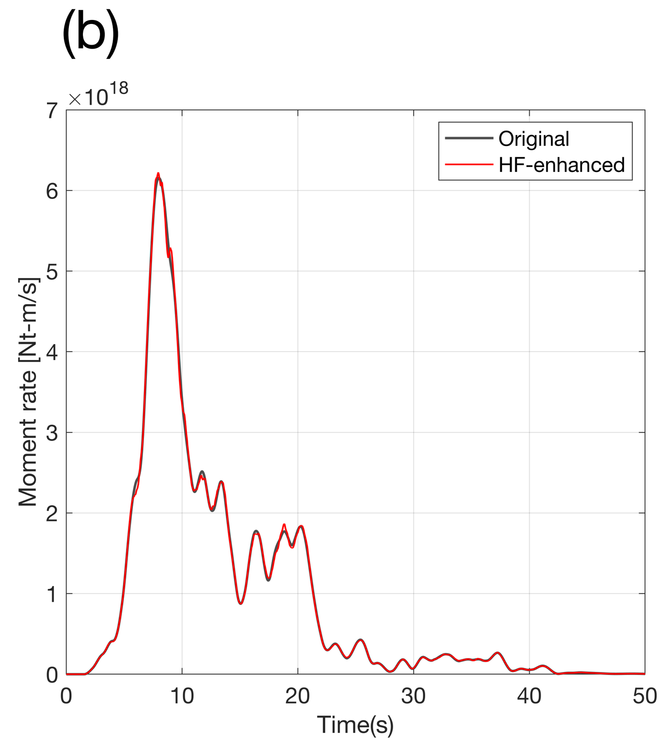

(c)

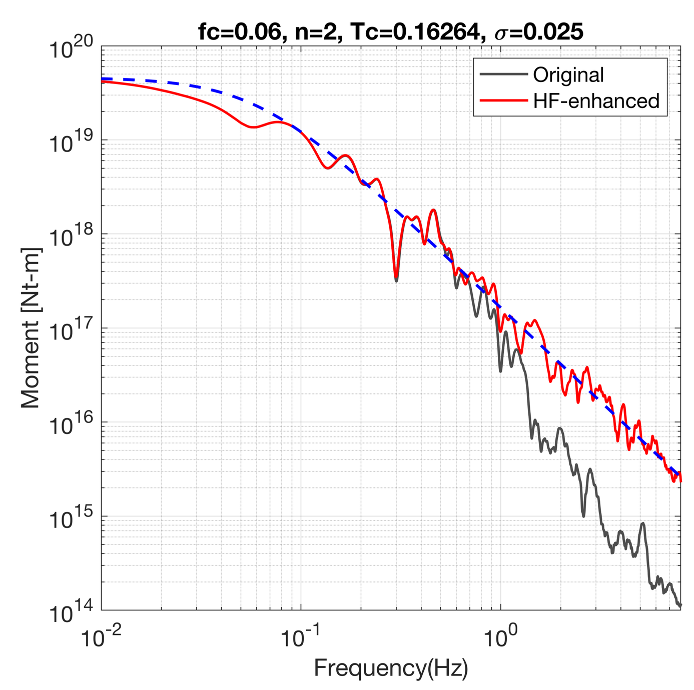

Surface topography

Figure (a): Topographic amplification = $\frac{PGV_{topo} - PGV_{nontopo}}{PGV_{nontopo}} \times 100\,\%$

Figures (b) and (c): Surface topography reduces PGAs and PGVs by ~21% and ~14% on average

Figure (d): Horizontal ground motions decrease by ~20% between 0.1-0.5 Hz, whereas vertical ground motions above 1Hz are enhanced by ~50% on average

Figure (e): Surface topography increases both significant velocity and acceleration durations

(a) Topographic amplification

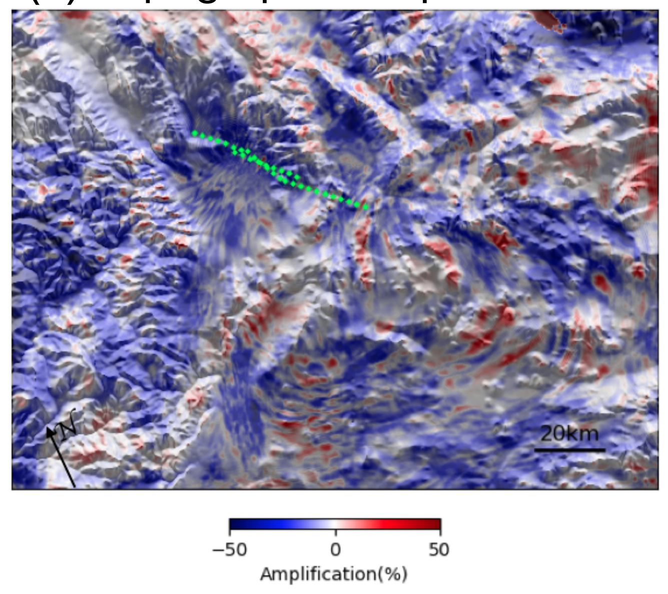

(b) PGV

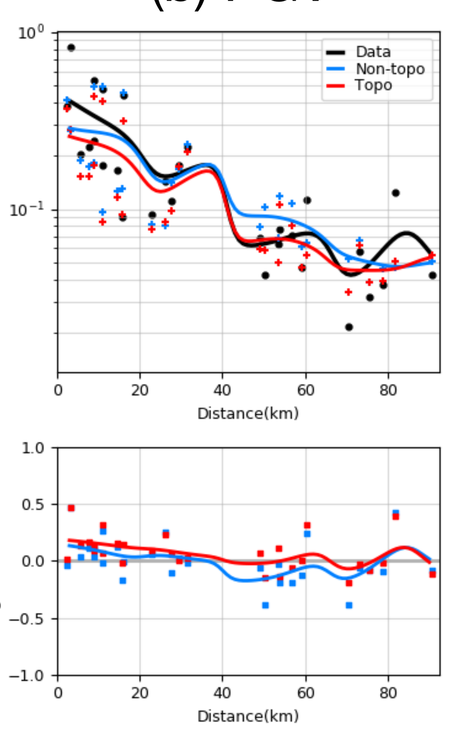

(c) PGA

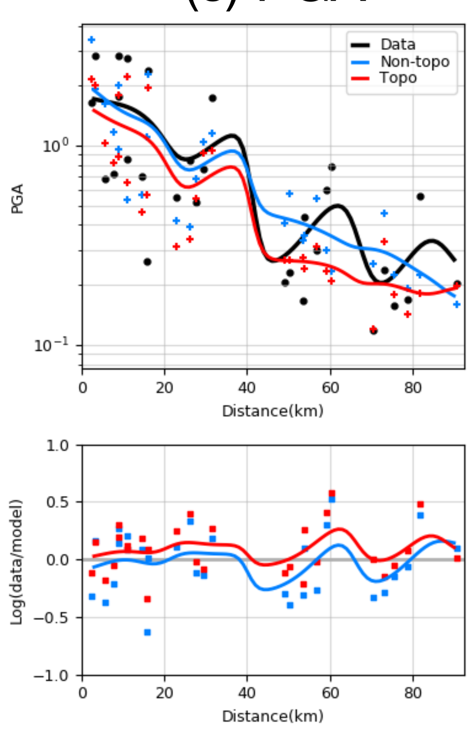

(d) Percent difference of velocity spectra

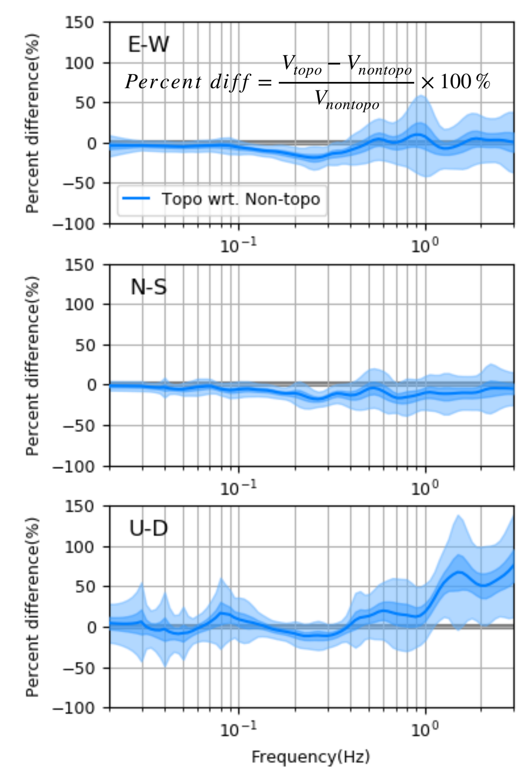

(e) 5-95% significant duration

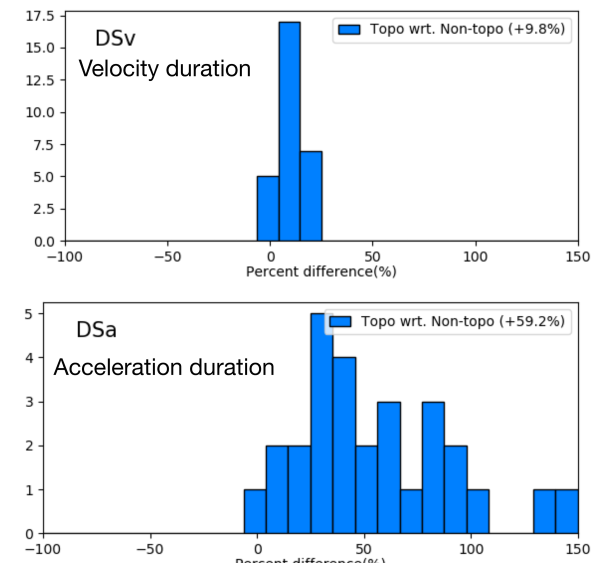

Small-scale heterogeneities

Including surface topography, from the surface to a depth of 5 km, we add 10% von Karman small-scale heterogeneities (SSHs). Correlation lengths=5km (horizontal) /1km (vertical) (**Figure a**).

Figures (b) and (c): SSHs reduce PGAs and PGVs by 7.4% and 6.8%, respectively.

Figure (d): Vertical-component PGAs and PGVs above 1Hz are enhanced by 30% on average while no significant difference can be seen on the horizontal components

Figure (e): Both velocity and acceleration durations are slightly increased

(a) Surface Vs

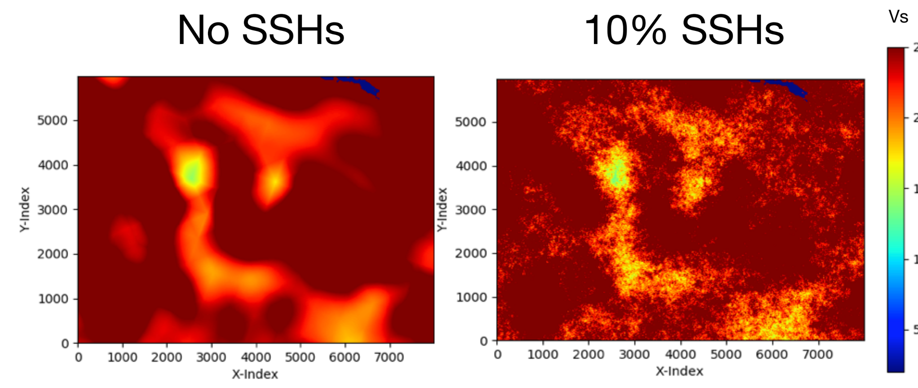

(b) PGV

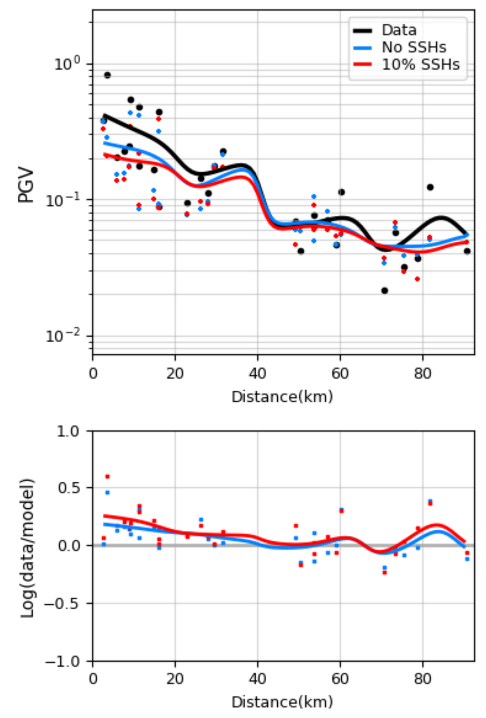

(c) PGA

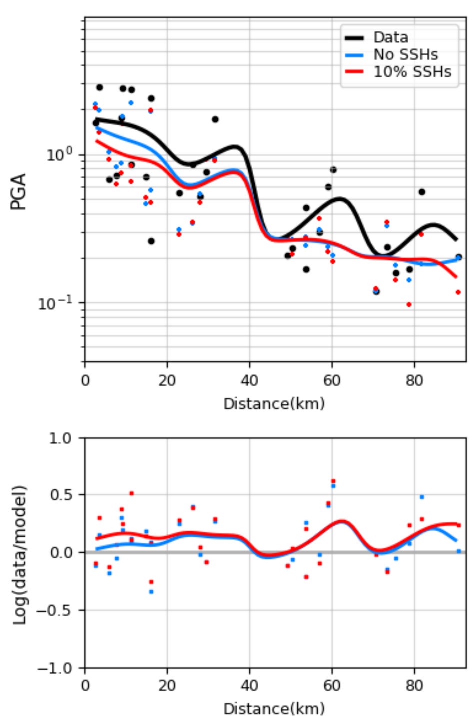

(d) Percent difference of velocity spectra

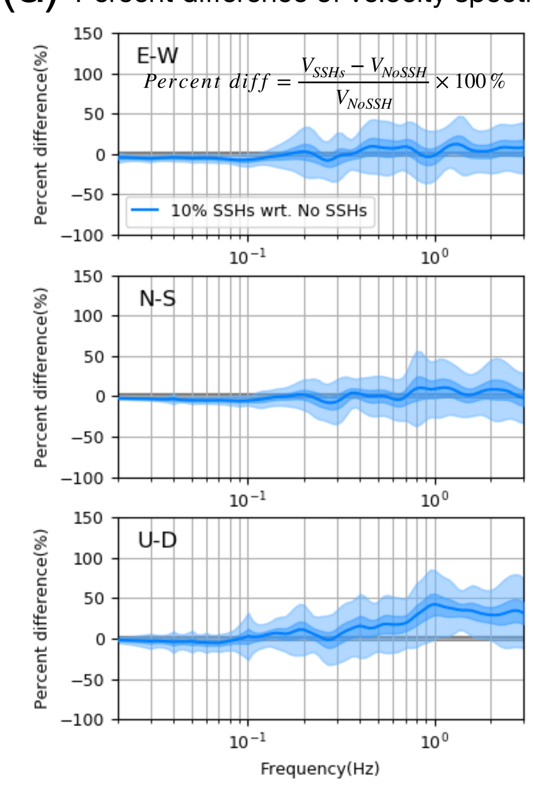

(e) 5-95% significant duration

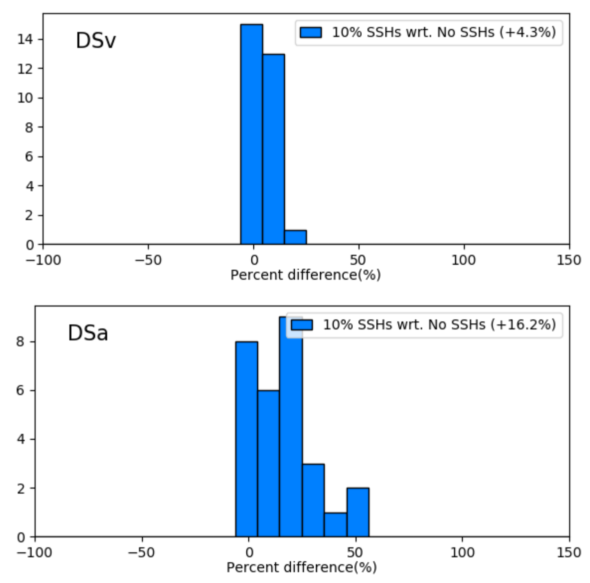

Conclusions

- We have tested the individual contributions of SSHs and surface topography on the ground motions from the 2019 M7.1 Ridgecrest earthquake.
- Both topography and SSHs decrease horizontal and increase vertical PGVs and PGAs above 1 Hz (Figure a).
- Both topography and SSHs increase the ground motion duration.
- With the assumption of 10% standard deviation of the SSHs, topography has a stronger effect of peak motions and durations for the Ridgecrest mainshock, as compared to SSHs.
- We demonstrate that including surface topography is essential since the non-topography model underpredicts the observed vertical ground motions above 1 Hz (Figure b).

(a) Percent difference w.r.t. Non-topo/No SSHs model

(b) Velocity spectral ratio against data

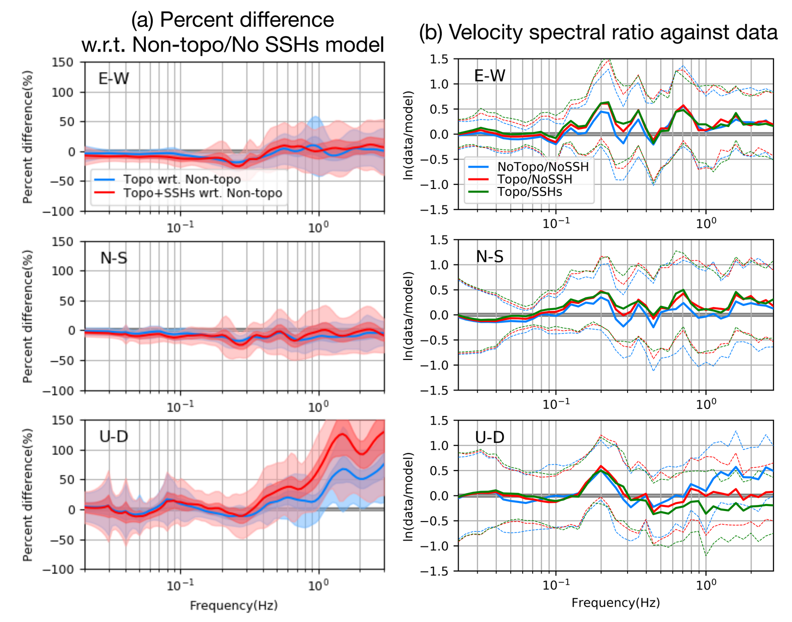

References

Liu, C., Lay, T., Brodsky, E. E., Dascher-Cousineau, K., & Xiong, X. (2019). Coseismic Rupture Process of the Large 2019 Ridgecrest Earthquakes From Joint Inversion of Geodetic and Seismological Observations. Geophysical Research Letters, 46(21), 11820-11829. https://agupubs.onlinelibrary.wiley.com/doi/abs/10.1029/2019GL084949

O'Reilly, O., Yeh, T. Y., Olsen, K. B., Hu, Z., Breuer, A., Roten, D., & Goulet, C. A. (2021). A High-Order Finite-Difference Method on Staggered Curvilinear Grids for Seismic Wave Propagation Applications with Topography. Bulletin of the Seismological Society of America. https://doi.org/10.1785/0120210096